Field-induced slow relaxation in a dinuclear dysprosium(III) complex based on 3-methoxycinnamic acid

Ouafa Khalfaoui, Adel Beghidja, Jérome Long, Chahrazed Beghidja, Yannick Guari, Joulia Larionova

inorganics

MDPI

Article

Field-Induced Slow Relaxation in a Dinuclear Dysprosium(III) Complex Based on 3-Methoxycinnamic Acid

Ouafa Khalfaoui [1], Adel Beghidja [1,*], Jérôme Long [2,*], Chahrazed Beghidja [1], Yannick Guari [2] and Joulia Larionova [2]

[1] Unité de Recherche de Chimie de l'Environnement et Moléculaire Structurale (CHEMS), Université Frères Mentouri Constantine, Route Aïn elbey, Constantine 25000, Algeria; khalfaoui.ouafa@yahoo.com (O.K.); cbeghidja@yahoo.fr (C.B.)

[2] Institut Charles Gerhardt Montpellier, UMR 5253, Ingénierie Moléculaire et Nano-Objects, Université de Montpellier, ENSCM, CNRS, Place E. Bataillon, 34095 Montpellier, France; yannick.guari@umontpellier.fr (Y.G.); joulia.larionova@umontpellier.fr (J.L.)

* Correspondence: a_beghidja@yahoo.fr (A.B.); jerome.long@umontpellier.fr (J.L.); Tel.: +213-5-4031-1190 (A.B.); +334-6414-3833 (J.L.)

Received: 29 November 2017; Accepted: 23 February 2018; Published: 20 March 2018

Abstract: We report the synthesis, structure, and magnetic properties of a new dinuclear dysprosium(III) complex based on a 3-methoxycinnamate ligand. The centrosymmetric complex exhibits a field-induced SMM behavior. In contrast to the previously reported lanthanide-based systems with cinnamate derivatives that relax through a combination of Raman and direct processes, an Orbach process is also involved in highlighting the role of the structural organization over the spin-lattice relaxations.

Keywords: lanthanide ions; single-molecule magnet; magnetic relaxation; single-crystal structure

1. Introduction

Slow relaxation of the magnetization in isolated lanthanide-based complexes and coordination polymers have been extensively studied since the discovery of a Single Molecule Magnets (SMM) behavior in mononuclear bis(phatlocyaninato) lanthanide complexes by Ishikawa and coll [1]. Such molecule-based compounds are often viewed as potential candidates for spintronics or high-density storage applications [2–5] since an important anisotropic barrier, Δ, may induce the appearance of a magnetic bistability. Recently, an important effort has been carried out to understanding the criteria governing the slow relaxation in SMM in order to optimize their behavior. Hence, numerous examples of complexes exhibiting large anisotropic barriers and magnetic bistability have been investigated in the last two years [6–10]. Among those, the observation of a magnetic hysteresis up to 60 K having the origin in the localized metal-ligand vibrational modes in a butyldysprosocenium complex constitutes an important breakthrough in this field and highlights the possibility to observe SMM behavior at relatively high temperatures [10]. In lanthanide-based SMM, the magnitude of the anisotropic barrier mainly depends on the ligand field splitting of lanthanide ions that is generated by the coordinated ligands [8,11]. This includes the stabilization of the 4f oblate or prolate electronic density of the lanthanides by specific ligands, as well as the Kramers/non-Kramers nature of the considered ion. The mechanism of the magnetic relaxation that allows for the flipping of the magnetization may have a complex origin and may proceed via the Quantum Tunneling of the Magnetization (QTM) and spin-phonon (lattice vibrations). The former depends on various parameters including deviation from high symmetry, dipolar interactions, hyperfine coupling, or

the presence of magnetic exchange interactions [12]. Thus, in polynuclear systems, the occurrence of magnetic intramolecular interactions could enhance the QTM [13]. In addition, the presence of different crystallographically independent lanthanide sites has been shown to favor the QTM through the appearance of a local transverse magnetic moment [13,14]. Nevertheless, exchange-biased systems have been shown to reduce the QTM [15–17] as highlighted in a dinuclear dinitrogen radical complex with a magnetic coercivity up to 14 K [18].

On the other hand, the "chemical criteria" affecting the spin-lattice relaxations are more difficult to comprehend and then to optimize in order to generate efficient systems. Intuitively, one variable that could strongly influence the spin-lattice vibrations concerns the dimensionality of the system. In this sense, examples of lanthanide-based Single-Chain Magnets are still rather limited. The reported examples include usually the association of lanthanide ions with either nitronyl nitroxide radical ligands [19,20] or carboxylate/phosphonate bridging ligands providing a relatively large separation between the spin carriers [21–29]. Owing to the large intra-chain Ln(III)–Ln(III) distances that are observed in these systems (from 4.83 to 8.99 Å), the magnetic relaxation has been ascribed to a single-ion relaxation rather than a cooperative behavior. However, this former might be also altered by the organization into extended structure with respect to molecular entities due to different spin-lattice relaxations.

Recently, we have reported several examples of discrete and extended architectures based on an association of lanthanide ions (Ce^{3+}, Nd^{3+}, Gd^{3+}, Dy^{3+}) with two different derivatives of cinnamic acid (2-methoxycinnamic and 3-methoxycinnamic acids) [30]. While the use of 2-methoxycinnamic acid conducts to the formation of dinuclear complexes, the use of 3-methoxycinnamic acid induces the formation of one-dimensional coordination polymers. For all of the investigated compounds, the magnetic properties reveal a field-induced slow relaxation of the magnetization having the origin in the presence of Raman and direct relaxation processes. Noticeably, in the case of Dy^{3+} systems, the relaxation time for the one-dimensional (1-D) structure has been found greater than for the dinuclear complex despite closely related environments.

Following this study, we report in this article the synthesis, structure and magnetic properties of a new dinuclear Dy^{3+} complex incorporating the 3-methoxycinnamate ligand. The direct comparison with the previously reported systems allows to assess the role of the coordination environment and structural organization over the overall magnetization dynamics.

2. Results

2.1. Synthesis and Crystal Structure

The reaction between 3-methoxycinnamic acid (L) (3 eq.) and $DyCl_3 \cdot 5H_2O$ (1 eq.) in the presence of sodium hydroxide in a DMF/water mixture allows for the formation of colorless crystals after re-crystallization in DMSO. The crystals that usually form rapidly are a one-dimensional coordination polymer, which we previously reported [30]. Remarkably, we have found that the kinetics of crystallization constitutes an important parameter that can be used to provide a further degree of control. Hence, if the crystallization is stood for a longer time (one month), a different compound of formula $[Dy(L)_3(DMSO)(H_2O)]_2$ (**1**) is obtained, suggesting a dissolution and recrystallization process. The single crystal X-ray diffraction analysis indicates that **1** is a strictly dinuclear complex that crystallizes in the triclinic $\overline{P}1$ space group (Table S1). The asymmetric unit consists in one crystallographically independent Dy^{3+} ion and three L^- ligands. The molecular arrangement is reminiscent that the dinuclear complexes obtained with the 2-methoxycinnamic acid [30]. The structure of **1** can be described as two nine-coordinated Dy^{3+} ions that are related via an inversion center and which are linked by six carboxylate groups from six L^- anions. One DMSO and one water molecule complete the lanthanide's coordination sphere Figure 1 (Top). Two different coordination modes of the carboxylate are observed in the structure: η^2 chelating and μ^2: $\eta^2-\eta^1$ chelating bridging modes. The Dy–O distances are ranging from 2.336(4) to 2.616(4) Å (Table S2) and the Dy^{3+}–O–Dy^{3+} bridging

angle is equal to 113.0(1)°. The intermetallic distance between two bridged Dy^{3+} ions is equal to 4.1311(6) Å. The in-depth analysis of the coordination geometry was performed using the SHAPE software [31] and can be described as a spherical capped square antiprism (Table S4). The analysis of the crystal packing reveals the presence of both, intra and intermolecular hydrogen-bonding interactions (Table S3) involving the carboxylate moieties and coordinated water molecules, resulting in the formation of a one-dimensional hydrogen bonded supramolecular structure. The shortest intermolecular Dy(III)–Dy(III) distance is found to be 6.183(1) Å.

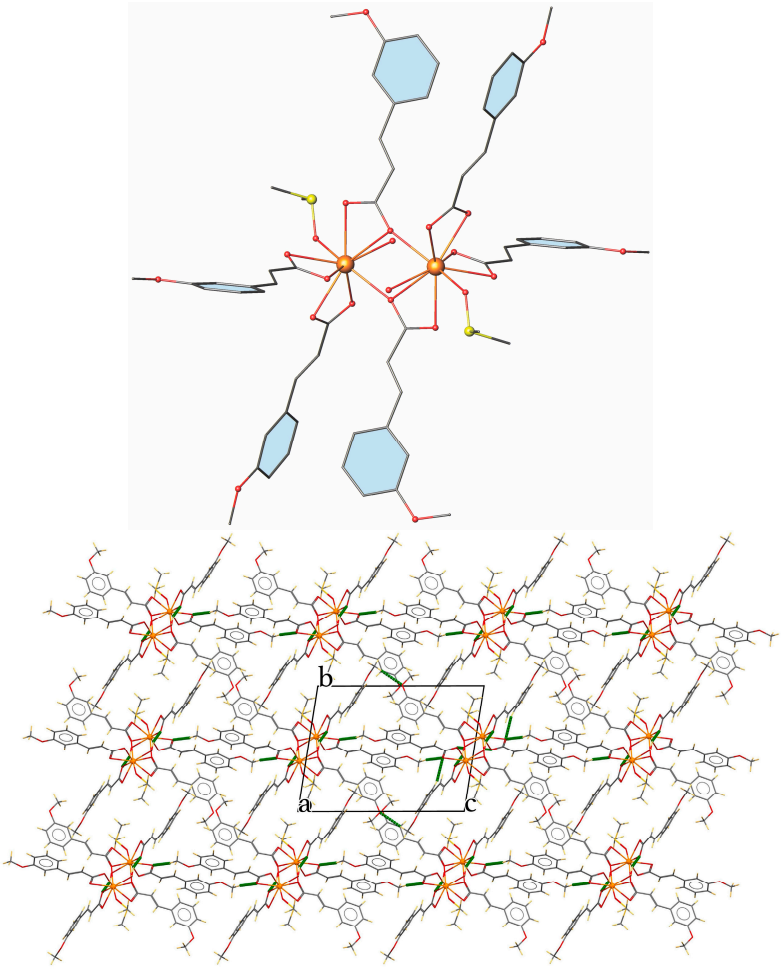

Figure 1. Top: Molecular structure of **1**. Color code: orange Ln, yellow S, red O, grey C. Hydrogen atoms have been omitted for clarity. Bottom: Packing arrangement of **1** viewed along the *a* crystallographic axis. The hydrogen bonding is indicated by green dashed lines.

2.2. DC Magnetic Properties

The room temperature value of χT equal to 27.51 $cm^3 \cdot K \cdot mol^{-1}$ is in a good agreement with the expected value of 28.24 $cm^3 \cdot K \cdot mol^{-1}$ for two non-interacting Dy^{3+} ions using the free-ion approximation. Upon cooling, χT remains constant down to 70 K before decreasing to reach the value of 17.31 $cm^3 \cdot K \cdot mol^{-1}$ at 1.8 K (Figure 2). Such deviation originates from the thermal depopulation of the Stark sublevels, which may be associated with dominant antiferromagnetic interactions between the two bridged Dy^{3+} ions. As previously evidenced in such carboxylate bridged systems, the strength of the magnetic interactions should be however relatively weak [15,30]. The field dependence of the magnetization measured at 1.8 K reaches the value of 12.77 μ_B under 70 kOe without evidence of a clear saturation (Inset of Figure 2).

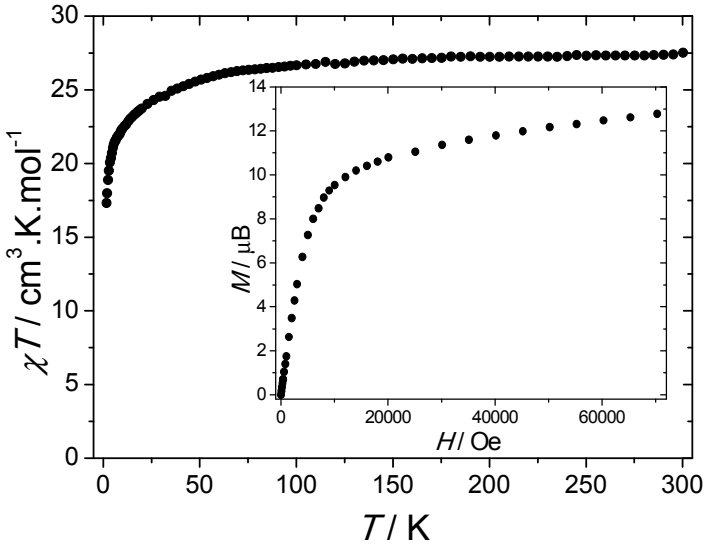

Figure 2. Temperature dependence of χT measured under a 1000 Oe DC field. Inset: field dependence of the magnetization measured at 1.8 K.

2.3. AC Magnetic Properties

AC magnetic properties were performed in order to investigate the occurrence of a slow relaxation of the magnetization. Under a zero DC field, a significant out-of-phase susceptibility signal, χ″, can be observed but without a maximum (Figure S1) due to the presence of a strong QTM, which may arise from external factors, such as dipolar interactions, intrinsic effects due to the hyperfine interactions, or symmetry deviations [12]. Applying DC field induces a short-cut of this QTM and a shift of the out-of-phase maximum towards lower frequencies. Thus, the frequency dependence of χ″ for various DC fields was performed. The highest relaxation time, τ, is found for 2250 Oe (Figure S1). For higher field values a second maximum starts to appear at low frequencies and a decrease of τ is observed and can be imputed to the presence of the direct process, which becomes predominant. The field dependence of the relaxation time can be modeled with the following equation [32]:

$$\tau^{-1} = DH^4T + B_1/(1 + B_2H^2) + K \quad (1)$$

The first term accounts for the direct process (for Kramers-ion), the second one stands for the QTM, while the last is a constant that is accounting for the field-independent thermally activated and Raman processes. Despite the presence of four different parameters, it was not possible to obtain a meaningful fit using this model, suggesting a more complex behavior.

The frequency dependence of χ″ for various temperatures under a 2250 Oe DC field reveals a frequency dependent asymmetric peak (Figure 3). Hence, a plateau that may be identified as a second relaxation process is observed at low frequencies. Yet, the slight frequency dependence of the signals suggests the occurrence of a second relaxation. Unfortunately, it was not possible to obtain single-crystals of the dysprosium complex diluted in a diamagnetic matrix precluding the in-depth determination of the role of dipolar and exchange interactions. On the other hand, the maximum of the frequency dependent peak shifts to higher temperatures upon an increasing frequency, which indicates a field-induced slow relaxation of the magnetization.

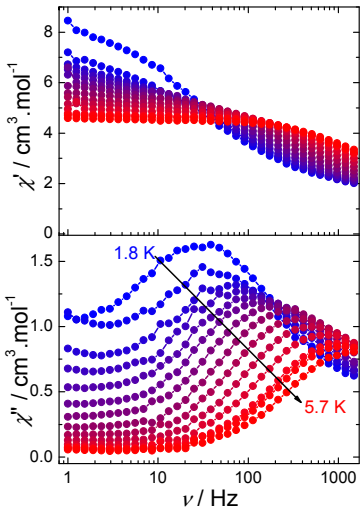

Figure 3. Frequency dependence of the in-phase (χ′) and out-of-phase (χ″) components of the ac susceptibility under an optimal magnetic DC field of 2250 Oe for **1**. Solid lines are guides to the eye.

The presence of a second relaxation process at low temperature is further corroborated when drawing the Cole–Cole plots (Figure 4a) exhibiting a plateau. Therefore, the Cole–Cole plots were fitted by taking into account only the data of the semi-circle corresponding to the high-temperature process (Table S5). Despite this, the α parameter values are ranging between 0.152 and 0.871, confirming a wide distribution of the relaxation times. Additional insights into the mechanism of the slow relaxation of the magnetization can be obtained by studying the temperature dependence of τ (Figure 4b). The deviation from the thermally activated behavior observed at low temperature indicates the occurrence of additional relaxation processes, such as Raman and/or direct. Fitting the temperature dependence of the relaxation time was performed using the following model [33]:

$$\tau^{-1} = {\tau_0}^{-1} \cdot \exp(-\Delta/kT) + CT^{m} + AT^{n} \quad (2)$$

for which the first term accounts for a thermally activated process, such as the Orbach or direct spin-phonon transitions involving higher excited states [8], while the second and third ones stand for two-phonon Raman and direct relaxation processes, respectively. To avoid the over-parameterization, the values of $m = 9$ and $n = 1$ were fixed to the values that were found for two-phonon Raman (for Kramers ions) and direct processes [34,35].

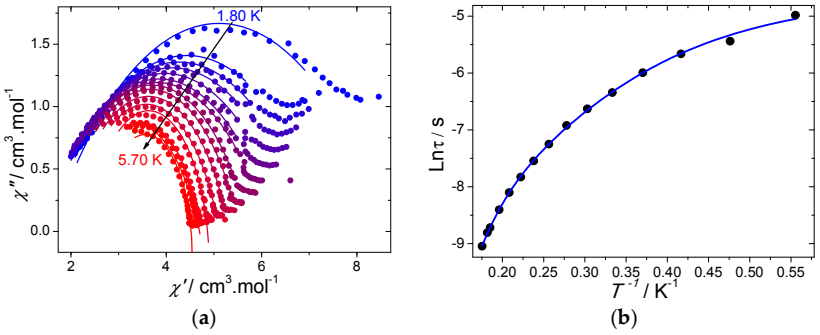

Figure 4. (**a**) Cole–Cole plots using the ac data performed under a 2250 Oe DC field for **1**. The solid lines correspond to the fit with a generalized Debye model; (**b**) Temperature dependence of the relaxation time using the ac data under a 2250 Oe DC field. The blue solid line corresponds to the fit with Equation (2).

The best fit parameters gave: $\Delta = 10 \pm 1$ cm^{-1}, $\tau_0 = (2.7 \pm 0.6) \times 10^{-6}$ s, $C = 0.0078 \pm 0.0003$ s^{-1}·K^{-9} and $A = 79 \pm 15$ s^{-1}·K^{-1}. The small value of Δ suggests a moderate contribution from

the Orbach process in this temperature range. Attempts to fit the temperature dependence of the relaxation time when considering only the Raman (*m* being free) and direct processes yields to lower correlation coefficient with respect to the fitting with Equation (2).

3. Discussion

Compound **1** behaves as a field-induced SMM with two relaxation processes. The occurrence of multiple relaxations has been widely observed in genuine field—induced lanthanide based SMM even in the case of one crystallographically relaxing lanthanide ion [11,13,36]. For **1**, the observed plateau at low frequencies most likely arises from a collective behavior resulting from strong dipolar interactions or from the occurrence of a hydrogen bonded network, as evidenced by the crystal structure analysis.

Further insights into the relaxation mechanism can be obtained through magneto-structural correlation. Based on the electrostatic model proposed by Rinehardt and Long [37], and latter extended by Chilton et al. [38], the efficient stabilization of the oblate electronic density of the Dy^{3+} ion could be achieved with an axial crystal field. This latter is highly dependent on the magnitude of the interaction between the negatively charged atoms of the ligand and the Dy^{3+} ion. For **1**, the two connected Dy^{3+} ions are related via an inversion center, inducing that the two anisotropic axes are collinear. However, the presence of six negatively charged or neutral oxygens atoms distributed homogeneously around the Dy^{3+} site is responsible from the deviation from axiality, promoting the QTM. This therefore explains the need to use a DC field to reduce this relaxation. The comparison with the previously reported dinuclear dysprosium-based complex involving the 2-methoxycinnamic acid derivative, as well as with the 1-D coordination polymer based on the 3-methoxycinnamic acid ligand [30] clearly sheds light on the role of the coordination environment and packing arrangement over the slow relaxation of the magnetization. While two relaxation processes have been evidenced in the dinuclear complex incorporating the 2-methoxycinnamate, the Orbach process was found negligible in contrast to Raman and direct processes. Thus, the relaxation time at 1.8 K is found to be one order of magnitude greater for **1** (Table 1, Figure S2), and the out-of-phase signals are observed up to higher temperatures. Similarly, the 1-D structure with the 3-methoxycinnamate ligands but with two crystallographically independent Dy^{3+} ions relaxes also via a combination of the Raman and direct processes, but the relaxation time remains three fold decreased with respect to **1**. This suggests that the organization of Dy^{3+} ions into the one-dimensional (1-D) structure does not improve the magnetic relaxation. Consequently, among these three compounds, the dinuclear complex **1** exhibits the best magnetic performances. As a result, the observed differences in the magnetic behavior of these compounds could be rather explained by subtle changes in the coordination environment of the Dy^{3+} sites. For instance, the different localization of the methoxy groups (H-bond acceptors) clearly generates different structural organizations that indirectly affects the first coordination sphere of the Dy^{3+} sites (Figure S3).

Table 1. Comparison of magnetic parameters for the different compounds.

Compound	Dimensionality	τ at 1.8 K (ms)	Δ (cm^{-1})	*m*	*C* ($s^{-1}\cdot K^{-m}$)	A($s^{-1}\cdot K^{-1}$)
$[Dy(L)_3(DMSO)(H_2O)]_2$ (**1**)	dinuclear complex	6.84	10 ± 1	9 *	0.0078 ± 0.0003	79 ± 15
$[Dy(L')_3(DMSO)(H_2O)]_2$	dinuclear complex	0.67	-	9 *	0.38 ± 0.02	983 ± 36
$[Dy_2(L)_6(DMSO)(H_2O)]_n\cdot DMF$	1-D structure	2.04	-	4.5 ± 0.2	3.6 ± 0.8	249 ± 12

L = 3-methoxycinnamate; L′ = 2-methoxycinnamate; * fixed parameter.

4. Materials and Methods

4.1. Synthesis and Crystal Structure

All of the chemicals were purchased from Alfa Aesar (Ward Hill, MA, USA) and were used as received. Single crystals of **1** were selected and measured on a Bruker-AXS APEX II CCD diffractometer (Bruker AXS Inc., Madison, WI, USA) at 293(2) K. The crystallographic data, conditions retained for the intensity data collection and some features of the structure refinements are listed

in Table S1. The intensities were collected with Mo Kα radiation (λ = 0.71073 Å). Data processing, Lorentz-polarization were performed using APEX [39]. Empirical absorption corrections were carried out using the SADABS program supplied by Bruker [40]. The structure was solved by the direct methods and refined by full-matrix least-squares methods on F^2, using the *SHELXL*-2104 [41]. Some of the reflections have been omitted because their intensities were seriously affected by the beamstop. Reflections are counted for which theta <3 Degrees and (Fo**2–Fc**2)/sqrt(weight) < −10.0. Those reflections are better removed from the final refinement since they are in systematic error, program package. All non-hydrogen atoms were refined anisotropically. The hydrogen atoms were located from difference Fourier maps, assigned with isotropic displacement factors and included in the final refinement cycles by use of geometrical constraints. Molecular plots were performed with the ATOMS and Mercury programs [42,43]. Geometrical calculations were carried out with PLATON [44].

4.2. Magnetic Measurements

Magnetic susceptibility data were collected with a Quantum Design MPMS-XL SQUID magnetometer (San Diego, CA, USA) working between 1.8 and 350 K with the magnetic field up to 7 Tesla. The data were corrected for the sample holder and the diamagnetic contributions calculated from Pascal's constants. The AC magnetic suceptibility measurements were carried out in the presence of a 3 Oe oscillating field in zero or applied external DC field.

5. Conclusions

In this article, we have reported the synthesis and crystal structure of a new dinuclear dysprosium(III) complex based on a 3-methoxycinnamate ligands. We have found that the kinetics of crystallization could strongly affect the dimensionality of the structure. The centrosymmetric complex **1** exhibits a field-induced SMM behavior. In contrast to the previously reported systems with cinnamate derivatives that relax through a combination of the Raman and direct processes, the Orbach relaxation is also involved, highlighting the role of the structural organization over the spin-lattice relaxations.

Supplementary Materials: The following are available online at www.mdpi.com/2304-6740/6/1/35/s1, Cif and cif-checked files. Figure S1: Top: Field dependence of the out-of-phase susceptibility, χ", at 1.8 K for **1**. Bottom: Field dependence of the relaxation time. The red solid line represents the fit using Equation (1). Figure S2: Temperature dependence of the relaxation time for three different dysprosium compounds. Figure S3: Differences in the packing arrangement between the dinuclear complexes. Table S1: Crystal data, data collection and refinement details for **1**. Table S2: Bond lengths and bond angles for **1**. Table S3: Hydrogen-bond geometry (Å, °). Table S4: SHAPE analysis. Table S5: Fitting of the Cole–Cole plots with a generalized Debye model for temperature ranging from 1.8 to 5.7 K under a 2250 Oe DC field for **1**.

Acknowledgments: The authors thank the University of Montpellier, CNRS, PAC ICGM and MESRS (Algeria) for financial supports.

Author Contributions: All authors contribute equally to this work. Ouafa Khalfaoui synthesized compound **1**. Adel Beghidja and Chahrazed Beghidja solved the crystal structure. Joulia Larionova performed the magnetic characterization. Adel Beghidja and Jérôme Long wrote the draft of the article. Yannick Guari and Joulia Larionova discussed the results and implications and commented on the manuscript at all stages.

Conflicts of Interest: The authors declare no conflict of interest.

References

1. Ishikawa, N.; Sugita, M.; Ishikawa, T.; Koshihara, S.-Y.; Kaizu, Y. Lanthanide double-decker complexes functioning as magnets at the single-molecular level. *J. Am. Chem. Soc.* **2003**, *125*, 8694–8695. [CrossRef] [PubMed]
2. Luzon, J.; Sessoli, R. Lanthanides in molecular magnetism: So fascinating, so challenging. *Dalton Trans.* **2012**, *41*, 13556–13567. [CrossRef] [PubMed]
3. Woodruff, D.N.; Winpenny, R.E.P.; Layfield, R.A. Lanthanide single-molecule magnets. *Chem. Rev.* **2013**, *113*, 5110–5148. [CrossRef] [PubMed]

4. Troiani, F.; Affronte, M. Molecular spins for quantum information technologies. *Chem. Soc. Rev.* **2011**, *40*, 3119–3129. [CrossRef] [PubMed]
5. Bogani, L.; Wernsdorfer, W. Molecular spintronics using single-molecule magnets. *Nat. Mater.* **2008**, *7*, 179–186. [CrossRef] [PubMed]
6. Liu, J.; Chen, Y.-C.; Liu, J.-L.; Vieru, V.; Ungur, L.; Jia, J.-H.; Chibotaru, L.F.; Lan, Y.; Wernsdorfer, W.; Gao, S.; et al. A stable pentagonal bipyramidal Dy(III) single-ion magnet with a record magnetization reversal barrier over 1000 K. *J. Am. Chem. Soc.* **2016**, *138*, 5441–5450. [CrossRef] [PubMed]
7. Gupta, S.K.; Rajeshkumar, T.; Rajaraman, G.; Murugavel, R. An air-stable Dy(III) single-ion magnet with high anisotropy barrier and blocking temperature. *Chem. Sci.* **2016**, *7*, 5181–5191. [CrossRef]
8. Ungur, L.; Chibotaru, L.F. Strategies toward high-temperature lanthanide-based single-molecule magnets. *Inorg. Chem.* **2016**, *55*, 10043–10056. [CrossRef] [PubMed]
9. Guo, F.S.; Day, B.M.; Chen, Y.C.; Tong, M.L.; Mansikkamaki, A.; Layfield, R.A. A dysprosium metallocene single-molecule magnet functioning at the axial limit. *Angew. Chem. Int. Ed. Engl.* **2017**, *56*, 11445–11449. [CrossRef] [PubMed]
10. Goodwin, C.A.P.; Ortu, F.; Reta, D.; Chilton, N.F.; Mills, D.P. Molecular magnetic hysteresis at 60 kelvin in dysprosocenium. *Nature* **2017**, *548*, 439–442. [CrossRef] [PubMed]
11. Liddle, S.T.; van Slageren, J. Improving f-element single molecule magnets. *Chem. Soc. Rev.* **2015**, *44*, 6655–6669. [CrossRef] [PubMed]
12. Pointillart, F.; Bernot, K.; Golhen, S.; Le Guennic, B.; Guizouarn, T.; Ouahab, L.; Cador, O. Magnetic memory in an isotopically enriched and magnetically isolated mononuclear dysprosium complex. *Angew. Chem. Int. Ed.* **2015**, *54*, 1504–1507. [CrossRef] [PubMed]
13. Blagg, R.J.; Ungur, L.; Tuna, F.; Speak, J.; Comar, P.; Collison, D.; Wernsdorfer, W.; McInnes, E.J.L.; Chibotaru, L.F.; Winpenny, R.E.P. Magnetic relaxation pathways in lanthanide single-molecule magnets. *Nat. Chem.* **2013**, *5*, 673–678. [CrossRef] [PubMed]
14. Moreno Pineda, E.; Chilton, N.F.; Marx, R.; Dörfel, M.; Sells, D.O.; Neugebauer, P.; Jiang, S.-D.; Collison, D.; van Slageren, J.; McInnes, E.J.L.; et al. Direct measurement of dysprosium(III)···dysprosium(III) interactions in a single-molecule magnet. *Nat. Comm.* **2014**, *5*, 5243. [CrossRef] [PubMed]
15. Long, J.; Habib, F.; Lin, P.-H.; Korobkov, I.; Enright, G.; Ungur, L.; Wernsdorfer, W.; Chibotaru, L.F.; Murugesu, M. Single-molecule magnet behavior for an antiferromagnetically superexchange-coupled dinuclear dysprosium(III) complex. *J. Am. Chem. Soc.* **2011**, *133*, 5319–5328. [CrossRef] [PubMed]
16. Katoh, K.; Asano, R.; Miura, A.; Horii, Y.; Morita, T.; Breedlove, B.K.; Yamashita, M. Effect of f-f interactions on quantum tunnelling of the magnetization: Mono- and dinuclear Dy(III) phthalocyaninato triple-decker single-molecule magnets with the same octacoordination environment. *Dalton Trans.* **2014**, *43*, 7716–7725. [CrossRef] [PubMed]
17. Xue, S.; Guo, Y.-N.; Ungur, L.; Tang, J.; Chibotaru, L.F. Tuning the magnetic interactions and relaxation dynamics of Dy_2 single-molecule magnets. *Chem. Eur. J.* **2015**, *21*, 14099–14106. [CrossRef] [PubMed]
18. Rinehart, J.D.; Fang, M.; Evans, W.J.; Long, J.R. Strong exchange and magnetic blocking in N_2^{3-}-radical-bridged lanthanide complexes. *Nat. Chem.* **2011**, *3*, 538–542. [CrossRef] [PubMed]
19. Bogani, L.; Sangregorio, C.; Sessoli, R.; Gatteschi, D. Molecular engineering for single-chain-magnet behavior in a one-dimensional dysprosium–nitronyl nitroxide compound. *Angew. Chem. Int. Edit.* **2005**, *44*, 5817–5821. [CrossRef] [PubMed]
20. Bernot, K.; Bogani, L.; Caneschi, A.; Gatteschi, D.; Sessoli, R. A family of rare-earth-based single chain magnets: Playing with anisotropy. *J. Am. Chem. Soc.* **2006**, *128*, 7947–7956. [CrossRef] [PubMed]
21. Wang, Y.; Li, X.-L.; Wang, T.-W.; Song, Y.; You, X.-Z. Slow relaxation processes and single-ion magnetic behaviors in dysprosium-containing complexes. *Inorg. Chem.* **2010**, *49*, 969–976. [CrossRef] [PubMed]
22. Tian, J.; Li, B.; Zhang, X.; Li, X.; Li, X.; Zhang, J. Three novel 1D lanthanide-carboxylate polymeric complexes: Syntheses, crystal structures and magnetic analyses. *Dalton Trans.* **2013**, *42*, 8504–8511. [CrossRef] [PubMed]
23. Bartolome, E.; Bartolome, J.; Melnic, S.; Prodius, D.; Shova, S.; Arauzo, A.; Luzon, J.; Luis, F.; Turta, C. $\{Dy(\alpha\text{-fur})_3\}_n$: From double relaxation single-ion magnet behavior to 3D ordering. *Dalton Trans.* **2013**, *42*, 10153–10171. [CrossRef] [PubMed]
24. Jung, J.; Le Natur, F.; Cador, O.; Pointillart, F.; Calvez, G.; Daiguebonne, C.; Guillou, O.; Guizouarn, T.; Le Guennic, B.; Bernot, K. Experimental and theoretical evidence that electrostatics governs easy-axis orientation in Dy(III)-based molecular chains. *Chem. Commun.* **2014**, *50*, 13346–13348. [CrossRef] [PubMed]

25. Chen, Q.; Meng, Y.-S.; Zhang, Y.-Q.; Jiang, S.-D.; Sun, H.-L.; Gao, S. A 1D dysprosium chain with slow magnetic relaxation constructed from a pyridine-*N*-oxide ligand. *Chem. Commun.* **2014**, *50*, 10434–10437. [CrossRef] [PubMed]
26. Huang, X.-C.; Zhang, M.; Wu, D.; Shao, D.; Zhao, X.-H.; Huang, W.; Wang, X.-Y. Single molecule magnet behavior observed in a 1-D dysprosium chain with quasi-D_{5h} symmetry. *Dalton Trans.* **2015**, *44*, 20834–20838. [CrossRef] [PubMed]
27. Holmberg, R.J.; Ho, L.T.A.; Ungur, L.; Korobkov, I.; Chibotaru, L.F.; Murugesu, M. Observation of unusual slow-relaxation of the magnetisation in a Gd-EDTA chelate. *Dalton Trans.* **2015**, *44*, 20321–20325. [CrossRef] [PubMed]
28. Han, T.; Leng, J.-D.; Ding, Y.-S.; Wang, Y.; Zheng, Z.; Zheng, Y.-Z. Field and dilution effects on the magnetic relaxation behaviours of a 1D dysprosium(III)-carboxylate chain built from chiral ligands. *Dalton Trans.* **2015**, *44*, 13480–13484. [CrossRef] [PubMed]
29. Holmberg, R.J.; Korobkov, I.; Murugesu, M. Enchaining EDTA-chelated lanthanide molecular magnets into ordered 1D networks. *RSC Adv.* **2016**, *6*, 72510–72518. [CrossRef]
30. Khalfaoui, O.; Beghidja, A.; Long, J.; Boussadia, A.; Beghidja, C.; Guari, Y.; Larionova, J. Cinnamic acid derivatives rare-earth dinuclear complexes and one-dimensionnal architectures: Synthesis, characterization and magnetic properties. *Dalton Trans.* **2017**, *46*, 3943–3952. [CrossRef] [PubMed]
31. Casanova, D.; Llunell, M.; Alemany, P.; Alvarez, S. The rich stereochemistry of eight-vertex polyhedra: A continuous shape measures study. *Chem. Eur. J.* **2005**, *11*, 1479–1494. [CrossRef] [PubMed]
32. Zadrozny, J.M.; Atanasov, M.; Bryan, A.M.; Lin, C.-Y.; Rekken, B.D.; Power, P.P.; Neese, F.; Long, J.R. Slow magnetization dynamics in a series of two-coordinate iron(II) complexes. *Chem. Sci.* **2013**, *4*, 125–138. [CrossRef]
33. Meihaus, K.R.; Minasian, S.G.; Lukens, W.W.; Kozimor, S.A.; Shuh, D.K.; Tyliszczak, T.; Long, J.R. Influence of pyrazolate vs *N*-heterocyclic carbene ligands on the slow magnetic relaxation of homoleptic trischelate lanthanide(III) and uranium(III) complexes. *J. Am. Chem. Soc.* **2014**, *136*, 6056–6068. [CrossRef] [PubMed]
34. Shrivastava, K.N. Theory of spin–lattice relaxation. *Phys. Status Solidi (b)* **1983**, *117*, 437–458. [CrossRef]
35. Scott, P.L.; Jeffries, C.D. Spin-lattice relaxation in some rare-earth salts at helium temperatures; observation of the phonon bottleneck. *Phys. Rev.* **1962**, *127*, 32–51. [CrossRef]
36. Amjad, A.; Figuerola, A.; Caneschi, A.; Sorace, L. Multiple magnetization reversal channels observed in a 3d-4f single molecule magnet. *Magnetochemistry* **2016**, *2*, 27. [CrossRef]
37. Rinehart, J.D.; Long, J.R. Exploiting single-ion anisotropy in the design of f-element single-molecule magnets. *Chem. Sci.* **2011**, *2*, 2078–2085. [CrossRef]
38. Chilton, N.F.; Collison, D.; McInnes, E.J.L.; Winpenny, R.E.P.; Soncini, A. An electrostatic model for the determination of magnetic anisotropy in dysprosium complexes. *Nat. Commun.* **2013**, *4*, 2551. [CrossRef] [PubMed]
39. *APEX3 and SAINT*, Version 3; Bruker AXS, Inc.: Madison, WI, USA, 2016.
40. *SADABS*, Version 2.03; Bruker AXS, Inc.: Madison, WI, USA, 2001.
41. Sheldrick, G. Crystal structure refinement with *SHELXL*. *Acta Cryst. C* **2015**, *71*, 3–8. [CrossRef] [PubMed]
42. Dowty, E. *Atoms*; Shape Software: Kingsport, TN, USA, 1999.
43. Macrae, C.F.; Edgington, P.R.; McCabe, P.; Pidcock, E.; Shields, G.P.; Taylor, R.; Towler, M.; van de Streek, J. Mercury: Visualization and analysis of crystal structures. *J. Appl. Cryst.* **2006**, *39*, 453–457. [CrossRef]
44. Spek, A. Structure validation in chemical crystallography. *Acta Cryst. D* **2009**, *65*, 148–155. [CrossRef] [PubMed]